

UC Davis

UC Davis Previously Published Works

Title

Sample seal-and-drop device and methodology for high temperature oxide melt solution calorimetric measurements of PuO₂.

Permalink

<https://escholarship.org/uc/item/2575302j>

Journal

The Review of scientific instruments, 90(4)

ISSN

0034-6748

Authors

Guo, Xiaofeng
Boukhalfa, Hakim
Mitchell, Jeremy N
[et al.](#)

Publication Date

2019-04-01

DOI




10.1063/1.5093567

Peer reviewed

Sample seal-and-drop device and methodology for high temperature oxide melt solution calorimetric measurements of PuO_2

Cite as: Rev. Sci. Instrum. **90**, 044101 (2019); <https://doi.org/10.1063/1.5093567>

Submitted: 22 February 2019 . Accepted: 28 March 2019 . Published Online: 19 April 2019

Xiaofeng Guo , Hakim Boukhalfa, Jeremy N. Mitchell , Michael Ramos, Andrew J. Gaunt, Albert Migliori, Robert C. Roback , Alexandra Navrotsky, and Hongwu Xu



View Online



Export Citation



CrossMark

AIP Author Services

English Language Editing

AIP
Publishing




Sample seal-and-drop device and methodology for high temperature oxide melt solution calorimetric measurements of PuO₂

Cite as: Rev. Sci. Instrum. 90, 044101 (2019); doi: 10.1063/1.5093567

Submitted: 22 February 2019 • Accepted: 28 March 2019 •

Published Online: 19 April 2019



Xiaofeng Guo,^{1,2,a)}  Hakim Boukhalfa,¹ Jeremy N. Mitchell,³  Michael Ramos,³ Andrew J. Gaunt,⁴ Albert Migliori,⁵ Robert C. Roback,¹  Alexandra Navrotsky,⁶ and Hongwu Xu^{1,a)}

AFFILIATIONS

¹Earth and Environmental Sciences Division, Los Alamos National Laboratory, Los Alamos, New Mexico 87545, USA

²Department of Chemistry and Alexandra Navrotsky Institute for Experimental Thermodynamics, Washington State University, Pullman, Washington 99164, USA

³Materials Science and Technology Division, Los Alamos National Laboratory, Los Alamos, New Mexico 87545, USA

⁴Chemistry Division, Los Alamos National Laboratory, Los Alamos, New Mexico 87545, USA

⁵National High Magnetic Field Laboratory, Los Alamos National Laboratory, Los Alamos, New Mexico 87545, USA

⁶Peter A. Rock Thermochemistry Laboratory and NEAT ORU, University of California Davis, Davis, California 95616, USA

^{a)}Electronic addresses: x.guo@wsu.edu and hxu@lanl.gov

ABSTRACT

Thermodynamic properties of refractory materials, such as standard enthalpy of formation, heat content, and enthalpy of reaction, can be measured by high temperature calorimetry. In such experiments, a small sample pellet is dropped from room temperature into a calorimeter operating at high temperature (often 700 °C) with or without a molten salt solvent present in an inert crucible in the calorimeter chamber. However, for hazardous (radioactive, toxic, etc.) and/or air-sensitive (hygroscopic, sensitive to oxygen, pyrophoric, etc.) samples, it is necessary to utilize a sealed device to encapsulate and isolate the samples, crucibles, and solvent under a controlled atmosphere in order to prevent the materials from reactions and/or protect the personnel from hazardous exposure during the calorimetric experiments. We have developed a sample seal-and-drop device (calorimetric dropper) that can be readily installed onto the dropping tube of a calorimeter such as the Setaram AlexSYS Calvet-type high temperature calorimeter to fulfill two functions: (i) load hazardous or air-sensitive samples in an air-tight, sealed container and (ii) drop the samples into the calorimeter chamber using an “off-then-on” mechanism. As a case study, we used the calorimetric dropper for measurements of the enthalpy of drop solution of PuO₂ in molten sodium molybdate (3Na₂O·4MoO₃) solvent at 700 °C. The obtained enthalpy of -52.21 ± 3.68 kJ/mol is consistent with the energetic systematics of other actinide oxides (UO₂, ThO₂, and NpO₂). This capability has thus laid the foundation for thermodynamic studies of other Pu-bearing phases in the future.

Published under license by AIP Publishing. <https://doi.org/10.1063/1.5093567>

I. INTRODUCTION

High temperature reaction calorimetry has versatile applications in studying the thermodynamic properties of materials, such as standard enthalpy of formation, heat capacity, heat content, and enthalpy of reaction. In particular, oxide melt solution calorimetry (in which a sample is equilibrated within a calorimeter at 700 or 800 °C and then stirred into a molten salt solvent) developed by Kleppa *et al.*^{1–3} and, later, oxide melt drop solution calorimetry (in which a

pelletized sample is dropped from room temperature into the molten salt solvent in the calorimeter, see Fig. 1) pioneered by Navrotsky^{4–6} provide accurate measurements of enthalpies of reactions for a variety of materials important to many research fields including chemistry, materials science, and geosciences.^{7–38} Recently, a comprehensive database of high temperature drop solution enthalpies (ΔH_{ds}) of oxide compounds has been published, based on decades-long calorimetric experiments of phases that contain elements across about 40% of the periodic table.⁶ These values can be used to

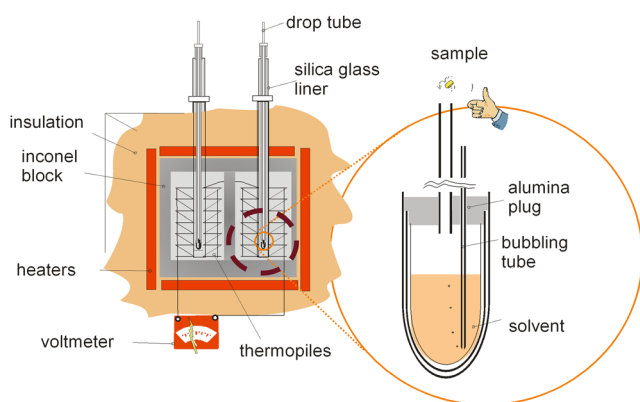


FIG. 1. Schematic of a high-temperature twin Calvet calorimeter and assembly for drop solution calorimetry in a molten oxide solvent.⁶

determine the enthalpies of formation from oxides ($\Delta H_{f,ox}$) and standard enthalpies of formation (ΔH_f°) from elements of ternary or more complex oxide systems.

Currently, there are two common solvents used in oxide melt drop solution calorimetry: sodium molybdate ($3\text{Na}_2\text{O}\cdot 4\text{MoO}_3$) and lead borate ($2\text{PbO}\cdot \text{B}_2\text{O}_3$). Although lead borate solvent can readily dissolve silicates, its use for other systems has been hampered by slow dissolution or limited solubility of oxides of large highly charged cations, potential reduction and deposition of Pb during calorimetric experiments involving reactions under reducing conditions, the toxicity of lead, and the need to use expensive crucibles (platinum or gold) to contain the solvent. At the same time as the lead borate solvent system was developed,³ a molten sodium molybdate solvent was also explored.^{4,5} Its lower toxicity, lack of corrosion of silica crucibles, and facile dissolution of a variety of oxides of large trivalent, tetravalent, and pentavalent cations has made it very useful for calorimetric studies involving these elements.^{5,6,35,36} The sodium molybdate solvent is also catalytic in oxidizing nitrides and sulfides to form dissolved oxides and sulfates, permitting determination of their enthalpies of formation.^{36,39–41}

The use of oxide melt drop solution calorimetry with the sodium molybdate solvent has proven to be a valuable technique in promoting lanthanide and actinide research, especially on light actinides (uranium, thorium), in terms of fundamental understanding of actinide bonding,^{30–32,42} probing the thermochemistry of uranyl minerals,^{17,33,43–46} interpreting nuclear fuel alteration,^{11,20,24,31,36} and predicting the long-term stability of actinide-immobilized solid waste matrices.^{19,22,23,25,28} These studies rely on accurate measurements of drop solution enthalpies of binary light-actinide-containing oxides, such as ThO_2 , UO_2 , U_3O_8 , and UO_3 .^{10,13,24,27,47} Recently, ΔH_{ds} values of NpO_2 and Np_2O_5 in molten $3\text{Na}_2\text{O}\cdot 4\text{MoO}_3$ have been reported.³⁵ However, no ΔH_{ds} value is available for PuO_2 in the literature, partly due to the safety (radiotoxicity) concerns and limited accessibility associated with Pu.

The lack of fundamental thermochemical parameters has hindered in-depth studies on thermodynamic properties, thermal stabilities, and environmental reactivities of Pu-containing compounds, which are critically needed for Pu research relevant to many

aspects of the nuclear enterprise. The knowledge gap in Pu thermodynamics motivated us to conduct drop-solution calorimetric measurements on Pu-bearing phases, starting with PuO_2 .

To safely perform Pu calorimetric measurements, we designed and fabricated a sample seal-and-drop device (which we call a calorimetric dropper) with two main functions: (i) loading and containing radioactive samples (and also for other hazardous or air/moisture-sensitive materials) in the sealed sample compartments; and (ii) dropping samples into the calorimeter chamber using an off-then-on mechanism after its installation onto a normal calorimetric setup (Fig. 1). Using two calorimetric droppers on the twinned Setaram AlexSYS calorimeter operating at 700°C , we successfully conducted drop solution calorimetry of three well characterized PuO_2 samples into molten $3\text{Na}_2\text{O}\cdot 4\text{MoO}_3$ at the Los Alamos National Laboratory (LANL). These experiments not only demonstrated the feasibility of the designed calorimetric dropper but also generated the ΔH_{ds} value for PuO_2 in the sodium molybdate solvent, which can be used for future calorimetric studies on other Pu-containing, more complex oxides.

II. DESIGN OF THE SAMPLE SEAL-AND-DROP DEVICE AND PROCEDURES FOR PU CALORIMETRIC EXPERIMENTS

A. Calorimetric dropper design

The assembled calorimetric dropper is shown in Figs. 2 and 3, and its components (shell, core, cap, shaft, and handle) are shown in Fig. 4. The shell, core, and cap can be made from various materials (e.g., steel, glass, ceramics, and plastics). Polyamide was used here as a raw material to fabricate the dropper by 3D printing. The shaft and handle are made of steel. The joints between components are connected and sealed using O-rings, particularly the one inside the cap that wraps the shaft and the other situated between the cap and shell so that the cap can be screwed onto the shell to seal the inside core. The O-rings are key components to ensure that the dropper is air-tight once assembled. One core has two spherical sample chambers (5 mm inner diameter), enough for holding a sample pellet or chunk (~ 2 mm in diameter). Figure 5 shows two functional modes of the device: one is the “off” mode for sealing the dropper and the other is the “on” mode to enable sample dropping. The dropper in

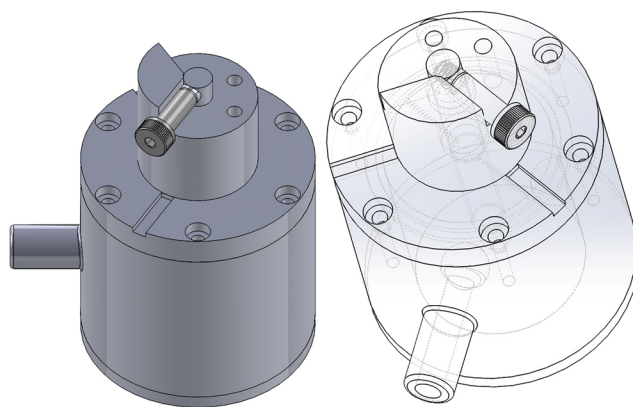


FIG. 2. Three-dimensional views of the assembled calorimetric dropper.

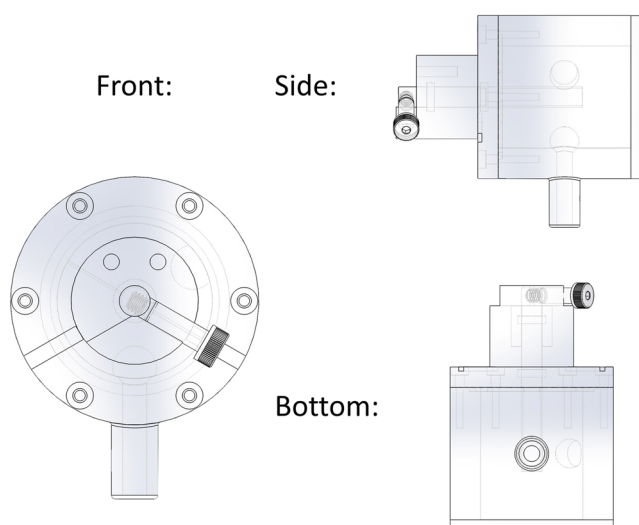


FIG. 3. Three views of the calorimetric dropper.

the “off” mode has the handle pointed up, which is the default position. The “off” mode is used when a sample-loaded dropper is in storage, during transportation, and when it is being installed on the dropping tube of a calorimeter. A safety fork is inserted into the cap

to lock the handle in the default “off” position (Fig. 3, front view), which is a safety feature that prevents accidental release of the loaded sample(s) from an unintended turning of the handle. The sealing mechanism of the dropper is realized by hooking the dropping tunnel with a commercially available two-way ball valve. Closing the ball valve makes the whole dropper air-tight. The final installation of the dropper to a calorimeter comes after attaching the other side of the valve to the dropping tube of the calorimeter, followed by opening the two-way ball valve so that the calorimeter can be connected to the core of the dropper via the dropping tunnel. To drop the samples into the calorimeter chamber (one at a time), guided by the dropping tunnel and the calorimeter dropping tube, one simply switches the handle to the “on” mode, as shown in Figs. 2 and 5. In the “on” mode, the handle is exactly at one of the terminal positions, beyond which it cannot pass (Fig. 5). Because the dropper is far outside the calorimeter, its manipulation has no effect on the calorimetric signal.

B. PuO_2 sample preparation and characterization

High purity PuO_2 powder (see Ref. 48 for synthesis and characterization details) was used as the starting material for creating a sintered PuO_2 pellet. The pellet was formed using a manual press with an internal diameter of $1/8''$. The extracted pellet was then sintered in a Netzsch 402C dilatometer under an ultrahigh purity (UHP) Ar atmosphere at 700°C for 15 min. Once cooled, the

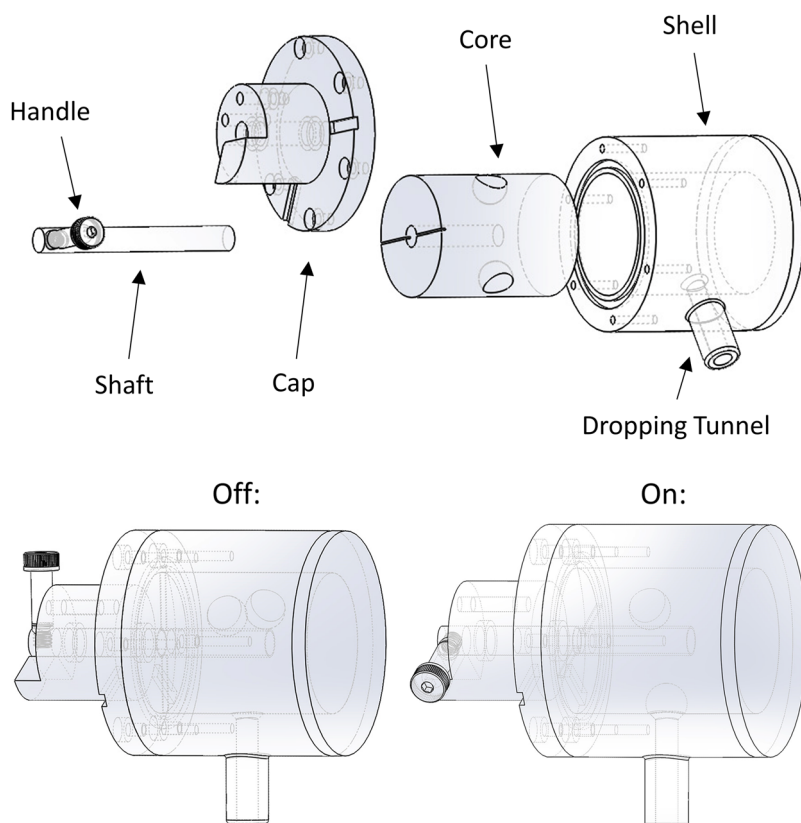


FIG. 4. Three-dimensional views of individual components of the calorimetric dropper.

FIG. 5. The “off” and “on” modes of the calorimetric dropper in perspective views.

sintered pellet was broken with a razor blade and small fragments were selected for drop-solution calorimetry.

C. Preparation in the calorimetry lab for Pu calorimetry

High temperature oxide melt drop solution calorimetry on PuO_2 was a four-day experiment conducted with a commercial Tian-Calvet twin microcalorimeter (Setaram Alexsys-800) operating at 700°C at LANL.^{29,34,36} Prior to the experiment, regular glassware setups for the calorimeter (Fig. 1) were assembled using two silica-glass sample crucibles with each containing ~ 15 g of sodium molybdate solvent. The $3\text{Na}_2\text{O}\cdot 4\text{MoO}_3$ powders first melted in the calorimeter at 700°C and then were removed and cooled to form a dense mass of solidified solvent prior to reinsertion in the calorimeter. All the glassware parts were hooked and sealed by vacuum grease; the gas ports on both glass liners, which normally serve as the exits for flushing gas, were closed by two high-efficiency particulate air (HEPA) filters to prevent potential release of airborne radioactive particles. The assembled glassware sets were inserted into the calorimeter, which became gradually stabilized over a period of ~ 12 h prior to the calorimetric experiment. Radiation protection and monitoring were set up around the calorimeter, including taping out an isolated radiological control area (RCA), monitoring the RCA with a real-time continuous air monitor (CAM), and implementing other safety protocols as stated in a detailed radiological work permit (RWP).

D. PuO_2 sample transportation and loading into calorimetric droppers

Since the PuO_2 sample was prepared in a distant radiological facility, a triple-contained PuO_2 sample package was shipped to another radiological laboratory close to the calorimeter. The package was unpacked, and the inner container containing PuO_2 sample fragments was transferred within a negative pressure UHP helium atmosphere glovebox designed for handling transuranic samples. The PuO_2 fragments were weighted by a semimicro balance and sequentially loaded into the sample compartments of two calorimetric droppers (Fig. 4). The two sample-loaded droppers were prewrapped with a parafilm prior to introduction into the glovebox to protect the exterior surfaces of the dropper from radiological contamination. After sample loading, the droppers were removed from the glovebox into an adjoining transuranic fume hood and the parafilm was removed followed by careful radiological surveys to ensure that the surfaces were free of contamination before exiting the radiological lab. Finally, the two contamination-free droppers were transferred to the calorimetry laboratory using designated containers for radioactive sample transportation.

TABLE I. Enthalpies of drop solution of PuO_2 in the molten sodium molybdate solvent at 700°C .

Compound	Weight (mg)	ΔH_{ds} (kJ/mol)
PuO_2 (Mass = 271.1 g/mol)	4.5	-54.82
	5.2	-53.81
	6.3	-47.99

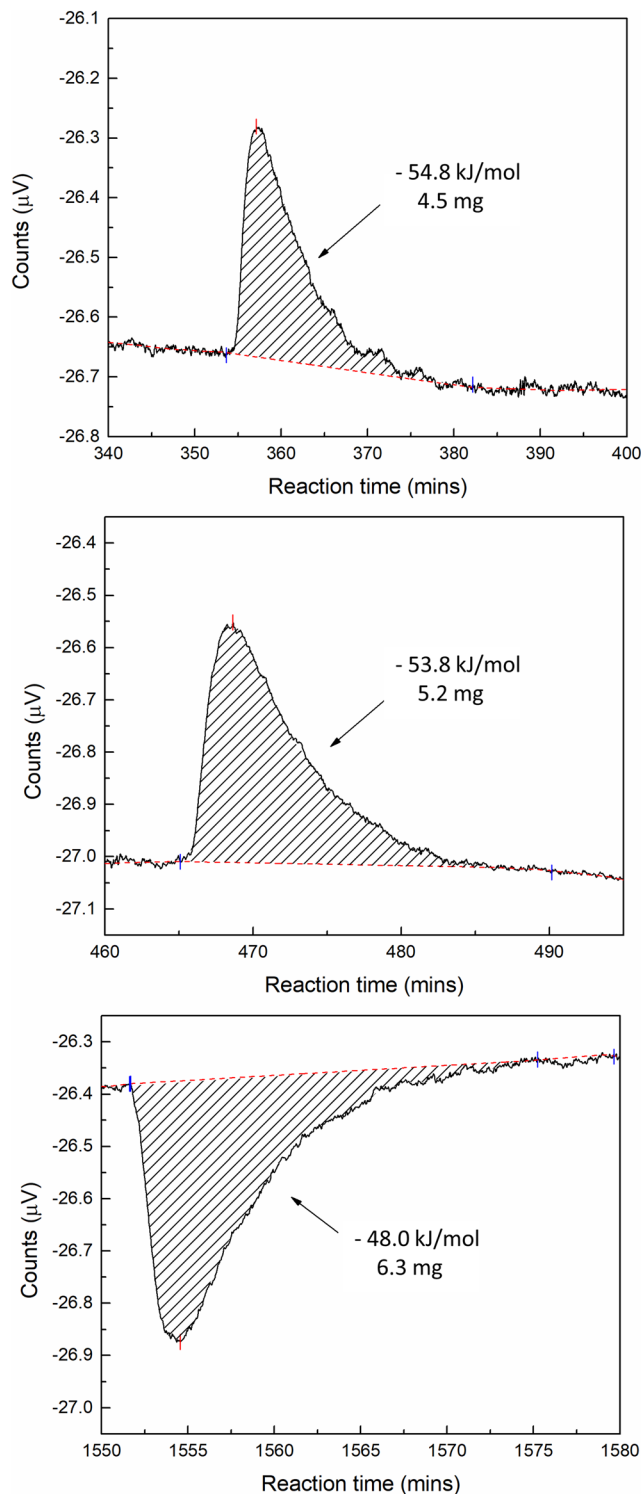


FIG. 6. Drop-calorimetric profiles of three PuO_2 pellets in the molten sodium molybdate solvent at 700°C . The first two profiles were produced from the reaction chamber in the left side of the calorimeter while the third profile was from the right. Signals collected from these two sides are opposite in sign so noise can be minimized to achieve high signal stability.

TABLE II. Enthalpies of drop solution of simple actinide oxides in the molten sodium molybdate solvent at 700 °C.

Actinide oxides	ΔH_{ds} (kJ/mol)
ThO ₂	0.89 ± 0.48 ¹³
UO ₂	−140.40 ± 2.67 ²⁷ −136.29 ± 2.34 ¹⁰
U ₃ O ₈	−79.02 ± 5.64 ^{a,24}
γ-UO ₃	9.49 ± 1.53 ¹⁰
am-UO ₃	−0.77 ± 0.06 ³¹
am-U ₂ O ₇	5.54 ± 1.52 ³¹
NpO ₂	7.81 ± 1.22 ³⁵
Np ₂ O ₅	34.22 ± 5.34 ³⁵
PuO ₂	−52.21 ± 3.68 ^b

^aThis value was obtained based on thermochemical data from the literature.^{10,50,56}

^bThis work.

E. Sealed high temperature drop solution calorimetry of PuO₂

The two sample-loaded calorimetric droppers were each installed on the top of one of the two dropping glass tubes of the calorimeter (Fig. 1) using the click-lock feature of the two-way ball valve (part of the dropper, see Sec. II C). After about a 1 h wait for calorimeter baseline stabilization, PuO₂ fragments were dropped sequentially (and alternately on the two sides of the calorimeter) from 25 °C into the calorimeter chambers at 700 °C using the “off-then-on” mechanism. The reaction and dissolution of the sample fragments in the sodium molybdate solvent produced three consistent ΔH_{ds} values of PuO₂ (Table I). Returning to the calorimeter baseline after ~30 min following each drop (Fig. 6) was a good indication that complete dissolution of PuO₂ was achieved. Full dissolution of the oxides of other actinides (U, Th, and Np) in the sodium molybdate solvent at 700 °C was reported previously, and their drop solution enthalpies were successfully obtained^{10,13,27,30,31,35} (Table II). The calorimetric peaks obtained with the dropper device were normal in all respects. In addition, no noticeable difference was observed in the obtained enthalpy value when the dropper was used in a monthly calorimeter calibration or in a drop solution calorimetric experiment on U₃Si₂.³⁶

F. Pu waste disposal after the calorimetric experiment

Upon completion of the calorimetric measurements, the two glassware/dropper sets were pulled out from the calorimeter in sequence. After each removal, the hot glassware/dropper set was immediately inserted into an Inconel waste cylinder, which was then sealed by an Inconel screwcap. Sealing of the two capped cylinders had been confirmed earlier by hydraulic tests. Alumina wool inside the cylinder serves as an insulation and buffering material to mitigate potential thermal and mechanical shocks upon inserting the glassware. The low thermal expansivity of silica glass minimizes thermal shock effects in the calorimetric assembly. During the entire process, the glassware/dropper sets remained intact. Finally, the two sealed, waste-loaded cylinders were shipped off-site for disposal under approved waste procedures.

III. RESULTS AND DISCUSSION

Calorimetric curves for the three PuO₂ fragments are plotted in Fig. 6, and the derived drop solution enthalpies (ΔH_{ds}) are listed in Table I. The mean ΔH_{ds} with the standard deviation is −52.21 ± 3.68 kJ/mol. For comparison, representative experimentally determined ΔH_{ds} values of simple actinide oxides are listed in Table II. Note that each ΔH_{ds} is a sum of several enthalpic components: (i) ΔH_{hc} , the heat content from 25 to 700 °C; (ii) ΔH_{ox} , the enthalpy of oxidation if the dissolved state has a different oxidation state from the initial solid (ThO₂, which does not have a ΔH_{ox} component); and (iii) ΔH_{soln} , the enthalpy of dissolution in the molten sodium molybdate at 700 °C. Determination of the contribution of ΔH_{soln} to ΔH_{ds} is needed to investigate whether the dissolving behavior of PuO₂ is consistent with those of other AnO₂ phases. First, ΔH_{hc} values of AnO₂ can be calculated from available high temperature heat capacity data (Table III). Second, determination of the enthalpy of oxidation requires the knowledge of the final state of the dissolved actinide species. The final valence states of U and Np in molten 3Na₂O·4MoO₃ are hexavalent^{10,27} and pentavalent,³⁵ respectively. Thus, ΔH_{ox} (UO₂) is derived to be −138.89 ± 3.08 kJ/mol, based on the oxidation reaction of UO₂ to γ-UO₃²⁷ at 700 °C, while ΔH_{ox} (NpO₂) is −3.85 kJ/mol, estimated from oxidizing NpO₂ to Np₂O₅.³⁵ The less exothermic ΔH_{ox} (NpO₂) compared with ΔH_{ox} (UO₂) is consistent with the observation that from U to higher actinides, the high oxidation state has a destabilization trend.^{35,49}

TABLE III. Breakdowns of the enthalpy of drop solution of AnO₂ in the molten sodium molybdate solvent (ΔH_{ds}) at 700 °C into the heat content from room temperature to 700 °C (ΔH_{hc}), enthalpy of oxidation (ΔH_{ox}), and enthalpy of solution (ΔH_{soln}).

AnO ₂	ΔH_{ds} (kJ/mol) ^a	ΔH_{hc} (kJ/mol)	ΔH_{ox} (kJ/mol)	ΔH_{soln} (kJ/mol)
ThO ₂	0.89 ¹³	49.50 ⁴⁹	...	−48.61
UO ₂	−138.35 ^{10,27}	52.80 ⁴⁹	−138.89 ⁵⁷	−52.26
NpO ₂	7.81 ³⁵	53.04 ⁴⁹	−3.85 ³⁵	−41.38
PuO ₂	−52.21 ^b	57.85 ⁴⁹	−55.2 ^c	−54.86 ^b

^aErrors not shown.

^bThis work.

^cEstimated based on the available literature data.^{49,50}

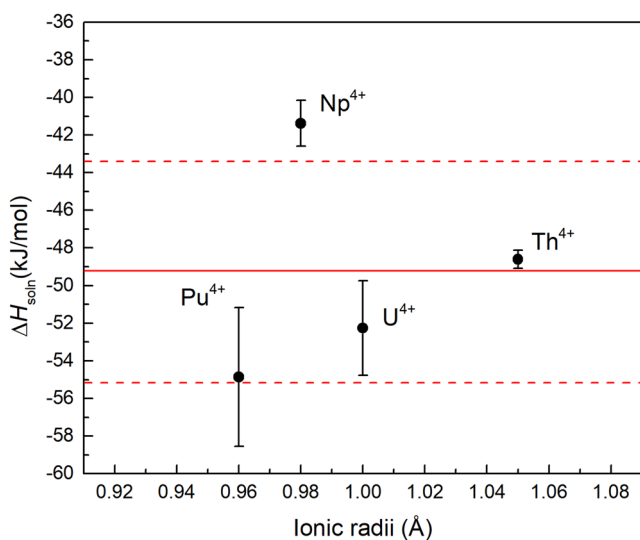


FIG. 7. Enthalpies of solution of AnO_2 ($\text{An} = \text{Th}, \text{U}, \text{Np},$ and Pu) in the molten sodium molybdate solvent at 700°C as a function of the ionic radius of An^{4+} .

The oxidation state of plutonium in the sodium molybdate solvent at 700°C in air has not yet been determined. We suspect that it may be between tetravalent and pentavalent since PuO_2 and Pu_4O_9 ^{49,52–54} are stable solid phases while Pu_2O_5 ⁵ is not. If Pu is tetravalent in the molten oxide solvent, then no further oxidation correction to the enthalpy of drop solution is needed. However, it results in a strongly negative enthalpy of solution value (-103.0 kJ/mol), not consistent with those of other AnO_2 (see Table III). If Pu is in mixed valence, we can take oxidation to Pu_4O_9 as a reference reaction. The oxidation enthalpy of this reaction can be approximated to be 0.575 eV/mol of Pu (or -55.2 kJ/mol of Pu), based on a computation by Korzhavyi *et al.*,^{50,51} which was used in this work for estimating $\Delta H_{\text{ox}}(\text{PuO}_2)$. Subtraction of $\Delta H_{\text{hc}}(\text{PuO}_2)$ ⁴⁹ and $\Delta H_{\text{ox}}(\text{PuO}_2)$ ^{49,50} from $\Delta H_{\text{ds}}(\text{PuO}_2)$ then gives $\Delta H_{\text{soln}}(\text{PuO}_2) = -54.86 \pm 3.68$ kJ/mol. Enthalpies of solution of ThO_2 , UO_2 , and NpO_2 are derived in a similar manner and listed in Table III. These ΔH_{soln} values are plotted in Fig. 7, where the mean with standard deviation of ΔH_{soln} values of these four AnO_2 phases (-49.28 ± 5.86 kJ/mol) is represented by a solid red line with upper and lower dashed line limits. Notably, our estimated $\Delta H_{\text{soln}}(\text{PuO}_2)$ falls well within the two limits, indicating a general consistency of our measured $\Delta H_{\text{ds}}(\text{PuO}_2)$ with all previously measured ΔH_{ds} of lighter actinide dioxides, supporting our assumption of the occurrence of mixed valence Pu in molten $3\text{Na}_2\text{O}\cdot 4\text{MoO}_3$. To refine this value, we plan to directly characterize the oxidation state of Pu in the solidified solvent after the dissolution of PuO_2 using synchrotron X-ray absorption spectroscopy.^{22,28,30,52} In addition, structural characterization (e.g., by synchrotron X-ray scattering and Raman spectroscopy at high T/P^{53–55}) will be conducted on AnO_2 series to establish its structure-energetics relationship.

IV. CONCLUSIONS

In this study, we present high temperature oxide melt drop solution calorimetric measurements of PuO_2 using our designed,

sample seal-and-drop device, along with a thorough protocol for handling transuranic samples during the experiment. The utilization of the calorimetric dropper enables a safe and reliable execution of such experiments with minimal risks of contamination. Moreover, the application of the dropper allows separation of the experiment into several tasks, which may be undertaken by different institutions or different divisions at a single institution. Notably, the application of the calorimetric dropper is not limited to the handling of transuranic samples. In general, the sealing mechanism of the dropper makes it possible to encapsulate samples that are hazardous (radioactive, toxic, etc.) or air-sensitive (hygroscopic, sensitive to oxygen, etc.) so that the personnel handling the samples can be properly protected from hazardous chemicals or the samples themselves can be prevented from reacting with air and/or moisture.

As an added outcome of the feasibility test of the calorimetric dropper, we obtained the drop solution enthalpy of PuO_2 in molten $3\text{Na}_2\text{O}\cdot 4\text{MoO}_4$ solvent at 700°C to be -52.21 ± 3.68 kJ/mol, which provides imperative information for future calorimetric studies of other Pu-containing phases and may serve as a benchmark value for related computational simulations. The approach developed in this work has thus laid the foundation for future drop-calorimetric measurements of the thermochemical parameters of transuranic compounds to fill the knowledge gap in actinide research.

ACKNOWLEDGMENTS

This work was supported by the Materials Science of Actinides (MSA), an Energy Frontier Research Center (EFRC), funded by the U.S. Department of Energy, Office of Science, Office of Basic Energy Sciences under Award No. DE-SC0001089, and the Laboratory Directed Research and Development (LDRD) program (Project No. 20180007 DR) of the Los Alamos National Laboratory (LANL). We thank Peter Burns for his support of this work through the MSA EFRC, and X.G. acknowledges the support through a LANL Seaborg postdoctoral fellowship and, later, the institutional funds from the Department of Chemistry at Washington State University. LANL, an affirmative action/equal opportunity employer, is managed by Triad National Security, LLC, for the National Nuclear Security Administration of the U.S. Department of Energy under Contract No. 89233218CNA000001.

REFERENCES

- 1 E. Calvet and H. Prat, *Recent Progress in Microcalorimetry* (Pergamon Press, Oxford, UK, 1963).
- 2 C. Colinet and A. Pasturel, in *Solution Calorimetry, Experimental Thermodynamics*, edited by K. N. Marsh and P. A. G. O'Hare (Blackwell, Oxford, 1994).
- 3 O. J. Kleppa, *J. Alloys Compd.* **321**, 153–156 (2001).
- 4 A. Navrotsky, *Phys. Chem. Miner.* **2**, 89–104 (1977).
- 5 A. Navrotsky, *Phys. Chem. Miner.* **24**, 222–241 (1997).
- 6 A. Navrotsky, *J. Am. Ceram. Soc.* **97**, 3349–3359 (2014).
- 7 H. W. Xu, A. Navrotsky, M. D. Nyman, and T. M. Nenoff, *J. Mater. Res.* **15**, 815–823 (2000).
- 8 H. Xu, A. Navrotsky, M. L. Balmer, Y. Su, and E. R. Bitten, *J. Am. Ceram. Soc.* **84**, 555–560 (2001).
- 9 M. L. Balmer, Y. Su, H. Xu, E. Bitten, D. McCready, and A. Navrotsky, *J. Am. Ceram. Soc.* **84**, 153–160 (2001).

- ¹⁰K. B. Helean, A. Navrotsky, E. R. Vance, M. L. Carter, B. Ebbinghaus, O. Krikorian, J. Lian, L. M. Wang, and J. G. Catalano, *J. Nucl. Mater.* **303**, 226–239 (2002).
- ¹¹K. A. H. Kubatko, K. B. Helean, A. Navrotsky, and P. C. Burns, *Science* **302**, 1191–1193 (2003).
- ¹²H. Xu, Y. Su, M. L. Balmer, and A. Navrotsky, *Chem. Mater.* **15**, 1872–1878 (2003).
- ¹³K. B. Helean, A. Navrotsky, G. R. Lumpkin, M. Colella, J. Lian, R. C. Ewing, B. Ebbinghaus, and J. G. Catalano, *J. Nucl. Mater.* **320**, 231–244 (2003).
- ¹⁴A. Navrotsky, H. Xu, E. C. Moloy, and M. D. Welch, *Am. Mineral.* **88**, 1612–1614 (2003).
- ¹⁵H. W. Xu, A. Navrotsky, M. L. Balmer, and Y. Su, *Phys. Chem. Miner.* **32**, 426–435 (2005).
- ¹⁶Q. Liu, H. Xu, and A. Navrotsky, *Microporous Mesoporous Mater.* **87**, 146–152 (2005).
- ¹⁷D. Gorman-Lewis, L. Mazeina, J. B. Fein, J. E. S. Szymanski, P. C. Burns, and A. Navrotsky, *J. Chem. Thermodyn.* **39**, 568–575 (2007).
- ¹⁸T. Varga, C. Lind, A. P. Wilkinson, H. Xu, C. E. Lesher, and A. Navrotsky, *Chem. Mater.* **19**, 468–476 (2007).
- ¹⁹K. Popa, T. Shvareva, L. Mazeina, E. Colineau, F. Wastin, R. J. Konings, and A. Navrotsky, *Am. Mineral.* **93**, 1356–1362 (2008).
- ²⁰C. R. Armstrong, M. Nyman, T. Shvareva, G. E. Sigmon, P. C. Burns, and A. Navrotsky, *Proc. Natl. Acad. Sci. U. S. A.* **109**, 1874–1877 (2012).
- ²¹G. C. Costa, H. W. Xu, and A. Navrotsky, *J. Am. Ceram. Soc.* **96**, 1554–1561 (2013).
- ²²X. Guo, A. H. Tavakoli, S. Sutton, R. K. Kukkadapu, L. Qi, A. Lanzirotti, M. Newville, M. Asta, and A. Navrotsky, *Chem. Mater.* **26**, 1133–1143 (2014).
- ²³X. Guo, Z. Rak, A. H. Tavakoli, U. Becker, R. C. Ewing, and A. Navrotsky, *J. Mater. Chem. A* **2**, 16945–16954 (2014).
- ²⁴X. Guo, S. V. Ushakov, S. Labs, H. Curtius, D. Bosbach, and A. Navrotsky, *Proc. Natl. Acad. Sci. U. S. A.* **111**, 17737–17742 (2014).
- ²⁵X. Guo, R. K. Kukkadapu, A. Lanzirotti, M. Newville, M. H. Engelhard, S. R. Sutton, and A. Navrotsky, *Inorg. Chem.* **54**, 4156–4166 (2015).
- ²⁶H. Xu, L. Wu, J. Zhu, and A. Navrotsky, *J. Nucl. Mater.* **459**, 70–76 (2015).
- ²⁷X. Guo, S. Szenknect, A. Mesbah, S. Labs, N. Clavier, C. Poinssot, S. V. Ushakov, H. Curtius, D. Bosbach, R. C. Ewing, P. C. Burns, N. Dacheux, and A. Navrotsky, *Proc. Natl. Acad. Sci. U. S. A.* **112**, 6551–6555 (2015).
- ²⁸X. Guo, A. Navrotsky, R. K. Kukkadapu, M. H. Engelhard, A. Lanzirotti, M. Newville, E. S. Ilton, S. Sutton, and H. Xu, *Geochim. Cosmochim. Ac.* **189**, 269–281 (2016).
- ²⁹H. W. Xu, M. E. Chavez, J. N. Mitchell, T. J. Garino, H. L. Schwarz, M. A. Rodriguez, D. X. Rademacher, and T. M. Nenoff, *J. Am. Ceram. Soc.* **98**, 2634–2640 (2015).
- ³⁰X. Guo, E. Tiferet, L. Qi, J. M. Solomon, A. Lanzirotti, M. Newville, M. H. Engelhard, R. K. Kukkadapu, D. Wu, E. S. Ilton, M. Asta, S. Sutton, H. Xu, and A. Navrotsky, *Dalton Trans.* **45**, 4622–4632 (2016).
- ³¹X. Guo, D. Wu, H. Xu, P. C. Burns, and A. Navrotsky, *J. Nucl. Mater.* **478**, 158–163 (2016).
- ³²X. Guo, C. Lipp, E. Tiferet, A. Lanzirotti, M. Newville, M. H. Engelhard, D. Wu, E. S. Ilton, S. Sutton, H. Xu, P. C. Burns, and A. Navrotsky, *Dalton Trans.* **45**, 18892–18899 (2016).
- ³³X. Guo, S. Szenknect, A. Mesbah, N. Clavier, C. Poinssot, D. Wu, H. W. Xu, N. Dacheux, R. C. Ewing, and A. Navrotsky, *Chem. Mater.* **28**, 7117–7124 (2016).
- ³⁴X. Guo and H. W. Xu, *J. Chem. Thermodyn.* **114**, 44–47 (2017).
- ³⁵L. Zhang, E. Dzik, G. Sigmon, J. Szymanski, A. Navrotsky, and P. Burns, *J. Nucl. Mater.* **501**, 398–403 (2017).
- ³⁶X. Guo, J. T. White, A. T. Nelson, A. Migdisov, R. Roback, and H. Xu, *J. Nucl. Mater.* **507**, 44–49 (2018).
- ³⁷H. Xu, *Nucl. Fuel Reprocess. Waste Manage.* **2**, 237 (2018).
- ³⁸L. Wu, J. Schliesser, B. F. Woodfield, H. Xu, and A. Navrotsky, *J. Chem. Thermodyn.* **93**, 1–7 (2016).
- ³⁹S. Elder, F. DiSalvo, L. Topor, and A. Navrotsky, *Chem. Mater.* **5**, 1545–1553 (1993).
- ⁴⁰J. M. McHale, A. Navrotsky, G. R. Kowach, and F. J. DiSalvo, *Chem.–Eur. J.* **2**, 1514–1517 (1996).
- ⁴¹S. Deore and A. Navrotsky, *Am. Mineral.* **91**, 400–403 (2006).
- ⁴²E. Tiferet, A. Gil, C. Bo, T. Y. Shvareva, M. Nyman, and A. Navrotsky, *Chem.–Eur. J.* **20**, 3646–3651 (2014).
- ⁴³T. Y. Shvareva, J. B. Fein, and A. Navrotsky, *Ind. Eng. Chem. Res.* **51**, 607–613 (2011).
- ⁴⁴A. Navrotsky, T. Shvareva, and X. Guo, in *Uranium – Cradle to Grave*, edited by P. C. Burns and G. E. Sigmon (Mineralogical Association of Canada, Winnipeg, MB, Canada, 2013) pp. 147–164.
- ⁴⁵M. Sharifronizi and P. C. Burns, *Can. Mineral.* **56**, 7–14 (2018).
- ⁴⁶M. Sharifronizi, J. E. Szymanski, J. Qiu, S. Castillo, S. Hickam, and P. C. Burns, *Inorg. Chem.* **57**, 11456–11462 (2018).
- ⁴⁷L. Zhang, A. Shelyug, and A. Navrotsky, *J. Chem. Thermodyn.* **114**, 48–54 (2017).
- ⁴⁸H. Yasuoka, G. Koutroulakis, H. Chudo, S. Richmond, D. Veirs, A. Smith, E. Bauer, J. Thompson, G. Jarvinen, and D. Clark, *Science* **336**, 901–904 (2012).
- ⁴⁹R. J. Konings, O. Beneš, A. Kovács, D. Manara, D. Sedmidubský, L. Gorokhov, V. S. Iorish, V. Yungman, E. Shenyavskaya, and E. Osina, *J. Phys. Chem. Ref. Data* **43**, 013101 (2014).
- ⁵⁰R. Guillaumont, T. Fanghanel, J. Fuger, I. Grenthe, V. Neck, D. A. Palmer, and M. H. Rand, *Update on the chemical thermodynamics of uranium, neptunium, americium, and technetium* (Elsevier, 2003) pp. 45–46.
- ⁵¹P. A. Korzhavyi, L. Vitos, D. A. Andersson, and B. Johansson, *Nat. Mater.* **3**, 225–228 (2004).
- ⁵²A. A. Migdisov, X. Guo, H. Xu, A. E. Williams-Jones, C. J. Sun, O. Vasyukova, I. Sugiyama, S. Fuchs, K. Pearce, and R. Roback, *Geochem. Perspect. Lett.* **5**, 47–52 (2017).
- ⁵³J. Zhang, A. Celestian, J. B. Parise, H. Xu, and P. J. Heaney, *Am. Mineral.* **87**, 566–571 (2002).
- ⁵⁴Z. Quan, Z. Luo, Y. Wang, H. Xu, C. Wang, Z. Wang, and J. Fang, *Nano Lett.* **13**, 3729–3735 (2013).
- ⁵⁵R. P. Li, J. Zhang, R. Tan, F. Gerdes, Z. P. Luo, H. W. Xu, J. A. Hollingsworth, C. Klinke, O. Chen, and Z. W. Wang, *Nano Lett.* **16**, 2792–2799 (2016).
- ⁵⁶M. W. J. Chase, *J. Phys. Chem. Ref. Data, Monogr.* **9**, 1–1951 (1998).
- ⁵⁷R. A. Robie and B. S. Hemingway, *U.S. Geol. Surv. Bull.* **2131**, 461 (1995).